# Adaptive Detection Probability for mmWave 5G SLAM

Henk Wymeersch* and Gonzalo Seco-Granados†
*Department of Electrical Engineering, Chalmers University of Technology, Sweden
†Department of Telecommunications and Systems Engineering, Universitat Autonoma de Barcelona, Spain
email: henkw@chalmers.se, gonzalo.seco@uab.cat

*Abstract*—In 5G simultaneous localization and mapping (SLAM), estimates of angles and delays of mmWave channels are used to localize the user equipment and map the environment. The interface from the channel estimator to the SLAM method, which was previously limited to the channel parameters estimates and their uncertainties, is here augmented to include the detection probabilities of hypothesized landmarks, given certain a user location. These detection probabilities are used during data association and measurement update, which are important steps in any SLAM method. Due to the nature of mmWave communication, these detection probabilities depend on the physical layer signal parameters, including beamforming, precoding, bandwidth, observation time, etc. In this paper, we derive these detection probabilities for different deterministic and stochastic channel models and highlight the importance of beamforming.

## I. INTRODUCTION

Wireless communication signals have an inherent relation to localization and mapping, as the received signals depend on the propagation environment and the location of the receiver with respect to the transmitter [1]. These properties are exploited explicitly in the GPS system, which extract time, Doppler, and phase measurements for localization of terrestrial users. Similarly, ultrawide bandwidth (UWB) communication systems are predominantly used for their high delay resolution, thanks to the massive UWB bandwidth [2]. Cellular communication systems have been relatively limited in their localization capabilities, predominantly for emergency call localization.

5G mmWave communication systems have several properties that make them attractive for user localization. The combination of large bandwidths and arrays with many elements lead to high delay and angular resolution. The operation at high carrier frequencies leads to sparse communication channels, further amplified by the use of directional beamforming [3]–[5]. These properties are also conducive for mapping, which is the determination of locations and properties of landmarks in the environment [6]. There is a rich literature on simultaneous localization and mapping (SLAM) in general [7]–[9] and more recently in radio-based SLAM in particular [10]–[12]. An important challenge in SLAM is the *data association* (DA) problem, which is the assignment of measurements to landmarks in the environment. DA considers every measurement as possibly being generated from every landmark, and makes hard [13] or soft [14] decisions based on the available statistical information.

Common to most SLAM methods is the implicitly layering of the problem. There is an underlying measurement process, which generates detections and with associated measurements (which include measurements from detected landmarks and measurements to due noise peaks, not corresponding to any physical landmark) with certain assumed statistics, with certain detection probabilities (i.e., the probability that a hypothesized landmark would lead to a measurement in a hypothesized user location). While layering is a sound engineering principle, care must be taken when defining the interfaces between the layers (i.e., the measurement process and the SLAM method). As we will see later, during DA, the detection probability plays a key role. Some existing methods consider this detection probability to be a constant [12], [15], either determined by the sensor field of view [11], or given a priori [10], [14]. Adaptive detection probabilities were proposed in [16] based on signal amplitude information, while [17] models the detection probability as a hidden random variable to be inferred. The above works do not consider the salient properties of 5G mmWave communication, where the detection probability depends on the physical layer signal parameters: bandwidth, observation time, signal structure, precoding, combining. In particular, the ability of mmWave to illuminate only parts of the propagation environment via beamforming and to only receive signals from certain directions is important to take into account. In addition, the detection probabilities depend on the applied channel estimation routine.

In this paper, we aim to quantify the detection probabilities used in 5G SLAM, in order to enrich the interface between the channel estimation routine and the SLAM algorithm. Our approach makes abstraction of the receiver signal processing, so our detection probabilities can be seen as optimistic upper bounds. We analyze the detection probability of several scenarios of interest, including line-of-sight (LOS) propagation, scattering from small objects, and reflection from large surfaces. Our results confirm the severe impact of the beamforming and the type of landmarks on the detection probabilities.

*Notation:* We denote estimates of a variable $x$ by $\hat{x}$ and hypothesized values of $x$ by $\tilde{x}$.

## II. MODEL

### A. Physical Layer Model

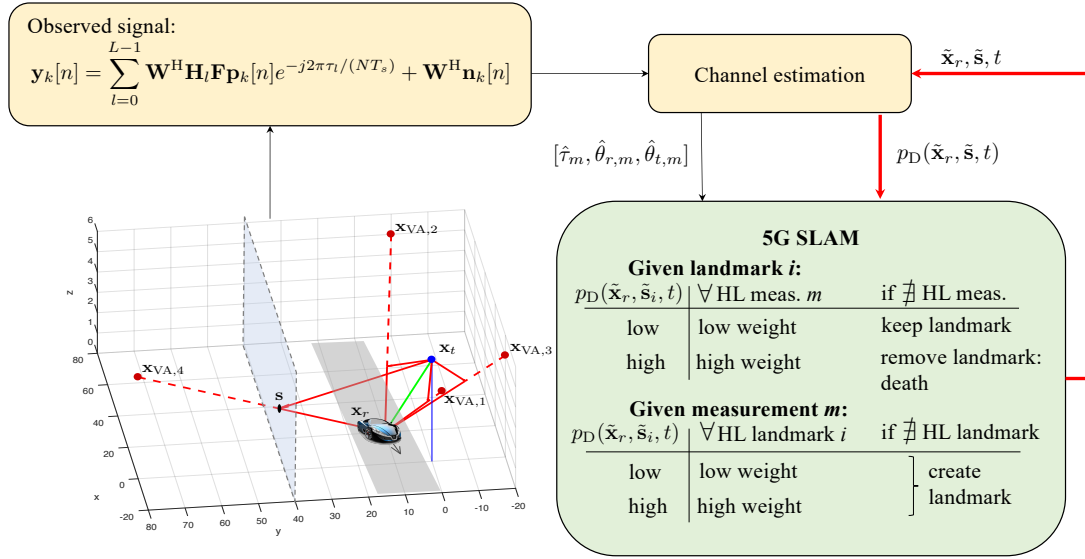We consider a 2D mmWave communication system with multiple paths, where the transmitter has $N_t$ antennas and

Figure 1. Concept: the standard interface between 5G SLAM and channel estimation is one-way, in the form of the channel parameters. The red arrows comprise the proposed augmentation to this interface, in order to provide 5G SLAM with correct detection probabilities. HL stands for high likelihood.

$M_t$ radio frequency (RF) chains, while the receiver has $N_r$ antennas and $M_r$ RF chains. To lighten the notation, we drop any indices related to mobility. The downlink signal is expressed as [18]

$$\mathbf{y}_k[n] = \sum_{l=0}^{L-1} \mathbf{W}^H \mathbf{H}_l \mathbf{F} \mathbf{p}_k[n] e^{-j2\pi\tau_l/(NT_s)} + \mathbf{W}^H \mathbf{n}_k[n], \quad (1)$$

where $l$ is the path index, $k \in \{0, \ldots, K-1\}$ is the transmissions index, $n \in \{0, \ldots, N-1\}$ is the subcarrier index, $\mathbf{W} \in \mathbb{C}^{M_r \times N_r}$ is a combining matrix at the receiver with $\mathbf{W}^H \mathbf{W} = \mathbf{I}_{M_r}$, $\mathbf{F} \in \mathbb{C}^{M_t \times N_t}$ is a precoding matrix at the transmitter with $\mathbf{F}^H \mathbf{F} = \mathbf{I}_{M_t}$, $\mathbf{p}_k[n]$ is the pilot at time $k$ on subcarrier $n$, $\mathbf{n}_k[n]$ is AWGN with covariance $N_0 \mathbf{I}_{N_t}$ (independent across transmission and subcarriers), $\tau_l$ is the time-of-arrival (TOA) of the $l$-th path and

$$\mathbf{H}_l = h_l \mathbf{a}_r(\theta_{r,l}) \mathbf{a}_t^T(\theta_{t,l}), \quad (2)$$

where $h_l \in \mathbb{C}$ is the complex channel gain with density $p(h_l)$, $\mathbf{a}_t(\theta_t)$ is the transmitter array response at angle-of-departure (AOD) $\theta_{t,l}$, and $\mathbf{a}_r(\theta_r)$ is the receiver array response at angle-of-arrival (AOA) $\theta_{r,l}$. Each path corresponds to a physical object/landmark in the environment, such as a reflecting surface or a scattering point. Path $l = 0$ denotes the LOS path (if it is present). We assume that objects are well separated, so that paths are also well separated in either TOA, AOD, or AOA [19]. We denote the location of the BS by $\mathbf{x}_t$, the location of the user by $\mathbf{x}_r$, and the location of an incidence point of a multipath component by $\mathbf{s}_l$.

*Remark* 1 (Simplified notation). For notational convenience and without loss of generality, we will consider the landmark location to be inter-changeable with the incidence point location $\mathbf{s}_l$. In general, the landmark may be different from the incidence point (e.g., a virtual anchor corresponding to a

reflecting surface). We also note that the BS and user location can also include their orientations, which affect the AOD and AOA, respectively, as well as a clock bias, which affects the TOA.

### B. 5G SLAM Model

As depicted in Figure 1, we further assume there exists a channel estimation routine, which determines an estimate of the number of paths $M$, where $M$ can be larger or smaller than $L$, the true number of paths. This estimate is based on a threshold, chosen to achieve a certain false alarm rate. For each detected path, the channel estimation routine also computes triples of channel parameters $\mathbf{z}_m = [\hat{\tau}_m, \hat{\theta}_{r,m}, \hat{\theta}_{t,m}]^T$, for $m = 0, \ldots, M-1$. These triples and their covariances are used in a 5G SLAM routine to localize the receiver and map the environment. A SLAM method includes a data association sub-routine, which aims to determine which channel parameters correspond to which object in the environment. Data association involves computation of association weights, $w_{m,i}$ for measurement $m$ and previously seen landmark $i > 0$ with estimated location $\tilde{\mathbf{s}}_i$ and are given[1] by [11], [20]

$$w_{m,i} = p_D(\tilde{\mathbf{x}}_r, \tilde{\mathbf{s}}_i, t) p(\mathbf{z}_m | \tilde{\mathbf{x}}_r, \tilde{\mathbf{s}}_i, t), \quad (3)$$

where $p_D(\tilde{\mathbf{x}}_r, \tilde{\mathbf{s}}_i, t)$ is the detection probability, i.e., the probability that a hypothesized object at position $\mathbf{s}_i$ would give rise to a measurement for a hypothesized user location $\tilde{\mathbf{x}}_r$. Here $t$ denotes the type of the path (e.g., LOS, reflecting surface, scatter point). The green box in Figure 1 shows the impact of the detection probability in 5G SLAM:

- For a given landmark $i$ of type $t$, if there is a measurement $m$ with high likelihood (HL) $p(\mathbf{z}_m | \tilde{\mathbf{x}}_r, \tilde{\mathbf{s}}_i, t)$ (marked HL

---

[1]This is a simplification of the true weight calculation in order to simplify the exposition. In addition, there are weights $w_{m,0}$ corresponding to new landmarks and $w_{0,i}$ corresponding to missed detections.

in Figure 1), then the association weight depends on the value of $p_D(\tilde{\mathbf{x}}_r, \tilde{\mathbf{s}}_i, t)$. In addition, if there is a high detection probability but no HL measurement, then the landmark should be removed from the map.

- We can also take the view from a given measurement $m$. If there is a HL landmark, then the weight will depend on the detection probability. If there is no HL landmark that can be associated with the measurement $m$, then a new landmark should be generated (a birth).

## III. DETECTION PROBABILITY DERIVATION

With the assumptions from Section II, we can focus on a single path, to compute $p_D(\tilde{\mathbf{x}}_r, \tilde{\mathbf{s}}, t)$, for a hypothesized receiver location $\tilde{\mathbf{x}}_r$, incidence point location $\tilde{\mathbf{s}}$, and object type $t$. For notational convenience we drop the index $i$.

### A. Derivation

Given these parameters, it is straightforward to compute the corresponding $[\tilde{\tau}, \tilde{\theta}_r, \tilde{\theta}_t]$, from basic 2D geometry [11]. In turn, given these parameters, we can consider the hypothetical observation

$$\tilde{\mathbf{y}}_k[n] = \tilde{h}\mathbf{W}^H\mathbf{a}_r(\tilde{\theta}_r)\mathbf{a}_t^T(\tilde{\theta}_t)\mathbf{F}\mathbf{p}_k[n]e^{-j2\pi\tilde{\tau}/(NT_s)} + \mathbf{W}^H\tilde{\mathbf{n}}_k[n], \tag{4}$$

where the channel gain has a density $p(\tilde{h}|\tilde{\mathbf{x}}_r, \tilde{\mathbf{s}}, t)$. We further denote $\tilde{\mathbf{p}}_k[n] = \mathbf{W}^H\mathbf{a}_r(\tilde{\theta}_r)\mathbf{a}_t^T(\tilde{\theta}_t)\mathbf{F}\mathbf{p}_k[n]e^{-j2\pi\tilde{\tau}/(NT_s)}$. We thus aim to determine whether a single path, leading to an observation (4) would lead to a detected or undetected path. The optimal processing would now proceed as follows:

1) Multiply $\tilde{\mathbf{y}}_k[n]$ with the complex conjugate of $\tilde{\mathbf{p}}_k[n]$, leading to observation

$$\tilde{z}_k[n] = \tilde{h}\|\tilde{\mathbf{p}}_k[n]\|^2 + \tilde{\mathbf{p}}_k^H[n]\mathbf{W}^H\tilde{\mathbf{n}}_k[n]. \tag{5}$$

2) Sum over all subcarriers and transmissions, leading to observation $\tilde{y} = \sum_{k,n} \tilde{z}_k[n]/\sqrt{N_0/2}$.

3) Consider as statistic $|\tilde{y}|^2$, which has a non-central $\chi^2$ distribution with 2 degrees of freedom and non-centrality parameter $2\tilde{P}|\tilde{h}|^2/N_0$, where $\tilde{P} = \sum_{k,n} \|\tilde{\mathbf{p}}_k[n]\|^2$

4) Given $\tilde{h}$ and a detection threshold $\gamma$, the conditional detection probability is given by

$$p_D(\tilde{\mathbf{x}}_r, \tilde{\mathbf{s}}, t|h) = p(|\tilde{y}|^2 > \gamma|\tilde{h}) \tag{6}$$

$$= Q_1\left(\sqrt{\frac{2\tilde{P}|\tilde{h}|^2}{N_0}}, \sqrt{\gamma}\right), \tag{7}$$

where $Q_1(\cdot, \cdot)$ is the Marcum Q-function.

5) The false alarm probability is related to $\gamma$ through

$$p_{FA} = p(|\tilde{y}|^2 > \gamma|\tilde{h} = 0) = e^{-\gamma/2}, \tag{8}$$

so that $\gamma = -2\log p_{FA}$.

The expected detection probability thus becomes

$$p_D(\tilde{\mathbf{x}}_r, \tilde{\mathbf{s}}, t) = \mathbb{E}_{\tilde{h}}\left\{Q_1\left(\sqrt{\frac{2\tilde{P}|\tilde{h}|^2}{N_0}}, \sqrt{\gamma}\right)\right\}, \tag{9}$$

where the expectation is with respect to the channel statistics with density $p(\tilde{h}|\tilde{\mathbf{x}}_r, \tilde{\mathbf{s}}, t)$. Observe that the detection probability does not depend on the observation $\tilde{y}$. In some cases, this integral can be computed analytically [21]. Note that when $|\tilde{h}| \to 0$, $p_D(\tilde{\mathbf{x}}_r, \tilde{\mathbf{s}}, t) \to p_{FA}$, so that $p_D \geq p_{FA}$.

*Remark* 2. When the transmitter and receiver are equipped with a single RF chain ($M_r = M_t = 1$), $\tilde{P}$ is given by

$$\tilde{P} = E_s KN\|\mathbf{w}^H\mathbf{a}_r(\tilde{\theta}_r)\mathbf{a}_t^T(\tilde{\theta}_t)\mathbf{f}\|^2 \leq E_s KNN_rN_t, \tag{10}$$

where $E_s$ is the energy per OFDM subcarrier, $K$ is the number of transmissions, and $N$ is the number of subcarriers. We observe the processing gain in time ($K$) and frequency ($N$), as well as the impact of beamforming, limited by $N_rN_t$.

### B. Application to mmWave Channels

In correspondence with the literature, we consider three special cases: the LOS path, a scatter point (SP), and a reflecting surface (represented by VA, for virtual anchor).

*1) Deterministic Models:* When the channel is deterministic the expectation over $\tilde{h}$ is omitted, so the detection probability depends on the deterministic value $|\tilde{h}|$. For $t = $ LOS, $\tilde{\mathbf{s}} = \emptyset$, and

$$|\tilde{h}| = \frac{\lambda}{4\pi\|\tilde{\mathbf{x}}_r - \mathbf{x}_t\|}, \tag{11}$$

where $\lambda$ is the wavelength of the signal at the carrier frequency; for $t = $ SP, the channel is governed by the radar equation [22]

$$|\tilde{h}| = \frac{\lambda\sqrt{S}}{(4\pi)^{3/2}\|\tilde{\mathbf{x}}_r - \tilde{\mathbf{s}}\|\|\tilde{\mathbf{s}} - \mathbf{x}_t\|}, \tag{12}$$

where $S$ is the object radar cross section (RCS). For $t = $ VA, the channel follows the reflection model

$$|\tilde{h}| = \frac{\lambda\Gamma}{4\pi(\|\tilde{\mathbf{x}}_r - \tilde{\mathbf{s}}\| + \|\tilde{\mathbf{s}} - \mathbf{x}_t\|)}, \tag{13}$$

where $0 \leq \Gamma \leq 1$ is the surface reflection coefficient.

*2) Stochastic Models:* The deterministic models can be augmented to include limited knowledge of the environment. For instance, for $t = $ LOS, the LOS path may be present with a certain probability $p_{LOS}$ [23]. The expectation in (9) is then with respect to the LOS probability:

$$p_D(\tilde{\mathbf{x}}_r, \tilde{\mathbf{s}}, \text{LOS}) = \tag{14}$$

$$p_{LOS}Q_1\left(\sqrt{\frac{2\tilde{P}\lambda^2}{16\pi^2\|\tilde{\mathbf{x}}_r - \mathbf{x}_t\|^2N_0}}, \sqrt{\gamma}\right) + (1 - p_{LOS})p_{FA}.$$

For $t = $ SP, the RCS may not be perfectly known and be drawn from a distribution $p(S)$, e.g., the well-known Swerling models [24]. Similarly, for $t = $ VA, the reflection coefficient may be characterized by $p(\Gamma)$, based on the material electromagnetic properties [25]. Another relevant case is fading for $t \neq $ LOS. Under Rayleigh fading, $p(\tilde{h}|\tilde{\mathbf{x}}_r, \tilde{\mathbf{s}}, t)$ follows a zero-mean Gaussian distribution, with variance determined by (12)–(13). Similarly, a Nakagami distribution can be considered for NLOS [26]. In all cases, the expectation is over a 1-dimensional variable, and can be computed using simple numerical techniques.
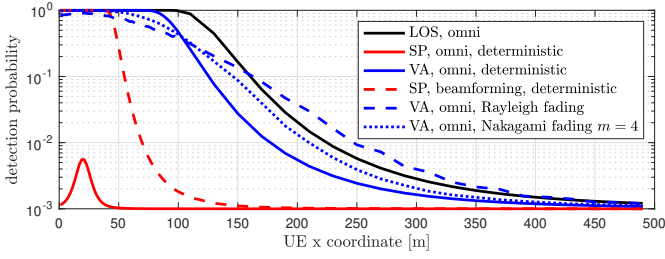
Figure 2. Detection probability as a function of the hypothesized UE location, $K = 1$, $p_{\text{FA}} = 0.001$.



Figure 3. Detection probability as a function of the hypothesized UE location for higher false alarm probability ($p_{\text{FA}} = 0.01$), $K = 1$.

## IV. RESULTS

### A. Scenario

We consider a scenario with a BS located at $\mathbf{x}_t = [0,0]^{\text{T}}$, sending $K = 1$ OFDM symbol with $N = 128$ subcarriers using an average transmit power of 1 mW, $N_0 = 4.0049 \times 10^{-9}$ mW/GHz, a total bandwidth of 200 MHz, and a carrier frequency of 28 GHz. Transmitter and receiver are equipped with ULAs with $N_t = N_r = 32$ antennas. There is a hypothesized incidence point at $\mathbf{s} = [20, 10]^{\text{T}}$, and a variable hypothesized user location $\tilde{\mathbf{x}}_r = [x_r, 0]^{\text{T}}$. We will visualize the detection probability as a function of $x_r$, for the LOS and and NLOS path, considering uniform precoding and combining, as well as directional precoding and combining. The precoding and combining matrices are columns from the DFT codebook, while the pilot data is constant[2] for all subcarriers (i.e., $\mathbf{p}_k[n] = \mathbf{p}, \forall k, n$). For the $t = $ SP hypothesis, $S = 10 \, \text{m}^2$, while for the $t = $ VA hypothesis, $\Gamma = 0.8$. We set $p_{\text{FA}} = 10^{-3}$, corresponding to $\gamma = 9.21$.

### B. Results and Discussion

Figure 2 shows the detection probabilities as a function of the hypothesized UE location, for six distinct scenarios. Four scenarios are without beamforming (labeled 'omni' in the figures), i.e., $M_t = N_t$, $M_r = N_r$, $\mathbf{F}$ and $\mathbf{W}$ are unitary $32 \times 32$ matrices. In one scenario there is beamforming, where $\mathbf{W}$ and $\mathbf{F}$ are a single column from the DFT matrix (i.e., $M_t = M_r = 1$).

- LOS path without beamforming: $p_{\text{D}}$ is around 1 for $x_r < 100 \, \text{m}$ since the signal is always much stronger than the noise, after which the detection probability degrades due to the path loss at large distances. At 160 m, $p_{\text{D}} \approx 0.1$.
- SP path without beamforming: in this case $p_{\text{D}}$ is always very small, with a peak of around 0.006 when the user is closest to the location $\tilde{\mathbf{s}}$. The low value of $p_{\text{D}}$ can be explained by the severe path loss in (12), essentially leading to the scatter point as a transmitter with power loss of $S/(4\pi\|\tilde{\mathbf{x}}_r - \tilde{\mathbf{s}}\|^2) \approx -14.5 \, \text{dB}$.
- VA path without beamforming: under the VA hypothesis, $p_{\text{D}}$ is similar to the LOS case, with some performance loss due to the additional path loss compared to the LOS

case. Roughly speaking, for the same $p_{\text{D}}$ the LOS path can be 40 m longer than the VA path.
- SP path with beamforming: we now consider the idealized case where the precoder chooses a column vector $\mathbf{f} = \mathbf{a}_t^*(\tilde{\theta}_t)/\|\mathbf{a}_t(\tilde{\theta}_t)\|$ and the combiner a column vector $\mathbf{w} = \mathbf{a}_r(\tilde{\theta}_r)/\|\mathbf{a}_r(\tilde{\theta}_r)\|$, in order to maximize the SNR gain. This leads to the red dashed curve. Now, for distances up to 40 m, $p_{\text{D}} \approx 1$, and then rapidly drops off. This clearly shows the importance of illuminating the environment, in order to achieve sufficient detection probability to enable SLAM.
- VA path without beamforming under Rayleigh fading: when the channel is random, generated according to a zero-mean distribution with power equal to the deterministic case above, we obtain the blue dashed curve. We notice that the fading reduces $p_{\text{D}}$ for $x_r < 100 \, \text{m}$, while for $x_r > 100 \, \text{m}$, $p_{\text{D}}$ is increased compared to the deterministic case. This effect can be ascribed to the shape of the Marcum Q-function.
- VA path without beamforming under Nakagami-$m$ fading (for $m = 4$): as show in the blue dotted curve, the Nakagami case is in between the Rayleigh and deterministic case. For $m = 1$, we find the Rayleigh results, while for $m \to +\infty$ we recover the deterministic curve.

To further boost the performance, we can increase $p_{\text{FA}}$ or send more consecutive OFDM symbols (increase $K$). Increase of $p_{\text{FA}}$ (shown in Figure 3) leads to some improvement of $p_{\text{D}}$ by raising the floor level, but will lead to more severe clutter for the SLAM algorithm, which in turn leads to higher complexity (each false path should be associated to each landmark) as well as ghost landmarks. On the other hand, Figure 4 shows the performance when we increase the coherent integration interval from $K = 1$ to $K = 10$ OFDM symbols. The additional SNR gain leads to orders of magnitude gains in detection probability and is the only meaningful way to discover small objects. However, care must be taken not to increase the coherent integration time beyond the coherence time of the channel.

## V. CONCLUSIONS

We have proposed a novel interface between mmWave channel estimation and 5G SLAM, by providing detection probabilities to the SLAM methods, based on the physical

---

[2]Note that this choice does not allow estimate of the DOA, but is selected for simplicity of the simulations and reduced stochasticity.

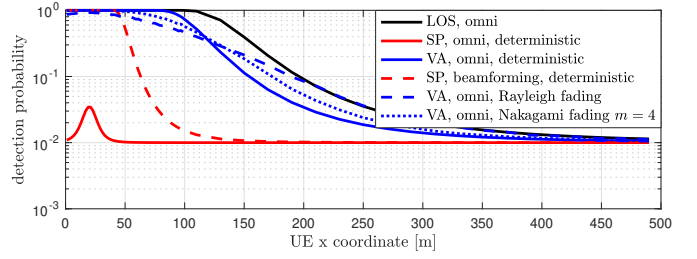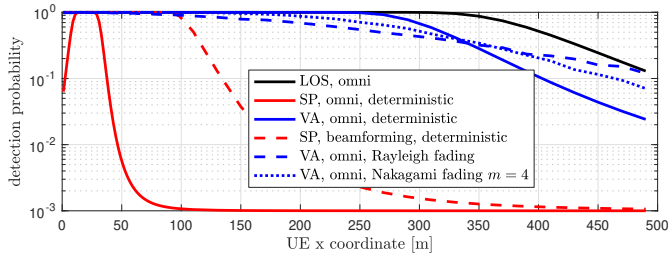Figure 4. Detection probability as a function of the hypothesized UE location for $K = 10$ OFDM symbols, $p_{\mathrm{FA}} = 0.001$.

layer signal parameters of the communication. We have derived simple expressions for the detection probability and applied these to a variety of propagation conditions. Our results indicate that beamforming and the coherent integration duration play a crucial role in the detection probability and should not be neglected in the SLAM. The proposed approach can also be used to guide system design, to meet certain quality metrics for SLAM, by modifying physical layer signal parameters to achieve certain target detection probabilities.

Possible avenues for future work include the impact of diffuse multipath and intelligent reconfigurable surfaces.

## ACKNOWLEDGMENTS

## REFERENCES

[1] J. Nurmi, E.-S. Lohan, H. Wymeersch, G. Seco-Granados, and O. Nykänen, *Multi-Technology Positioning*. Springer, 2017.

[2] Z. Sahinoglu, S. Gezici, and I. Guvenc, "Ultra-wideband positioning systems," *Cambridge, New York*, 2008.

[3] J. A. del Peral-Rosado, R. Raulefs, J. A. López-Salcedo, and G. Seco-Granados, "Survey of cellular mobile radio localization methods: From 1G to 5G," *IEEE Communications Surveys & Tutorials*, vol. 20, no. 2, pp. 1124–1148, 2017.

[4] K. Witrisal, P. Meissner, E. Leitinger, Y. Shen, C. Gustafson, F. Tufvesson, K. Haneda, D. Dardari, A. F. Molisch, A. Conti, *et al.*, "High-accuracy localization for assisted living: 5G systems will turn multipath channels from foe to friend," *IEEE Signal Processing Magazine*, vol. 33, no. 2, pp. 59–70, 2016.

[5] H. Wymeersch, G. Seco-Granados, G. Destino, D. Dardari, and F. Tufvesson, "5G mmwave positioning for vehicular networks," *IEEE Wireless Communications*, vol. 24, no. 6, pp. 80–86, 2017.

[6] R. Mendrzik, F. Meyer, G. Bauch, and M. Z. Win, "Enabling situational awareness in millimeter wave massive MIMO systems," *IEEE Journal of Selected Topics in Signal Processing*, vol. 13, no. 5, pp. 1196–1211, 2019.

[7] H. Durrant-Whyte and T. Bailey, "Simultaneous localization and mapping: part I," *IEEE Robotics & Automation Magazine*, vol. 13, no. 2, pp. 99–110, 2006.

[8] T. Bailey and H. Durrant-Whyte, "Simultaneous localization and mapping (SLAM): Part II," *IEEE Robotics & Automation Magazine*, vol. 13, no. 3, pp. 108–117, 2006.

[9] M. Adams, B.-N. Vo, R. Mahler, and J. Mullane, "SLAM gets a PHD: New concepts in map estimation," *IEEE Robotics & Automation Magazine*, vol. 21, no. 2, pp. 26–37, 2014.

[10] E. Leitinger, F. Meyer, F. Hlawatsch, K. Witrisal, F. Tufvesson, and M. Z. Win, "A belief propagation algorithm for multipath-based SLAM," *IEEE transactions on wireless communications*, vol. 18, no. 12, pp. 5613–5629, 2019.

[11] H. Kim, K. Granström, L. Gao, G. Battistelli, S. Kim, and H. Wymeersch, "5G mmwave cooperative positioning and mapping using multi-model PHD filter and map fusion," *arXiv preprint arXiv:1908.09806*, 2019.

[12] H. Naseri and V. Koivunen, "Cooperative simultaneous localization and mapping by exploiting multipath propagation," *IEEE Transactions on Signal Processing*, vol. 65, no. 1, pp. 200–211, 2016.

[13] M. Montemerlo, S. Thrun, D. Koller, B. Wegbreit, *et al.*, "FastSLAM 2.0: An improved particle filtering algorithm for simultaneous localization and mapping that provably converges," in *Int. Joint Conf. on Artificial Intelligence*, pp. 1151–1156, 2003.

[14] F. Meyer, T. Kropfreiter, J. L. Williams, R. Lau, F. Hlawatsch, P. Braca, and M. Z. Win, "Message passing algorithms for scalable multitarget tracking," *Proceedings of the IEEE*, vol. 106, no. 2, pp. 221–259, 2018.

[15] M. Fröhle, C. Lindberg, K. Granström, and H. Wymeersch, "Multisensor Poisson multi-Bernoulli filter for joint target-sensor state tracking," *IEEE Transactions on Intelligent Vehicles*, vol. 4, pp. 609–621, Dec 2019.

[16] E. Leitinger, S. Grebien, and K. Witrisal, "Multipath-based SLAM exploiting AoA and amplitude information," in *Proc. IEEE ICC-19*, 2019.

[17] E. Leitinger, F. Meyer, F. Tufvesson, and K. Witrisal, "Factor graph based simultaneous localization and mapping using multipath channel information," in *2017 IEEE International Conference on Communications Workshops (ICC Workshops)*, pp. 652–658, 2017.

[18] R. W. Heath, N. Gonzalez-Prelcic, S. Rangan, W. Roh, and A. M. Sayeed, "An overview of signal processing techniques for millimeter wave MIMO systems," *IEEE journal of selected topics in signal processing*, vol. 10, no. 3, pp. 436–453, 2016.

[19] Z. Abu-Shaban, X. Zhou, T. Abhayapala, G. Seco-Granados, and H. Wymeersch, "Error bounds for uplink and downlink 3d localization in 5g millimeter wave systems," *IEEE Transactions on Wireless Communications*, vol. 17, no. 8, pp. 4939–4954, 2018.

[20] B.-N. Vo and W.-K. Ma, "The gaussian mixture probability hypothesis density filter," *IEEE Transactions on signal processing*, vol. 54, no. 11, pp. 4091–4104, 2006.

[21] P. C. Sofotasios, M. Valkama, T. A. Tsiftsis, Y. A. Brychkov, S. Freear, and G. K. Karagiannidis, "Analytic solutions to a Marcum Q-function-based integral and application in energy detection of unknown signals over multipath fading channels," in *International Conference on Cognitive Radio Oriented Wireless Networks and Communications (CROWNCOM)*, pp. 260–265, 2014.

[22] A. Al-Hourani, R. J. Evans, S. Kandeepan, B. Moran, and H. Eltom, "Stochastic geometry methods for modeling automotive radar interference," *IEEE Transactions on Intelligent Transportation Systems*, vol. 19, no. 2, pp. 333–344, 2017.

[23] S. Sun, T. A. Thomas, T. S. Rappaport, H. Nguyen, I. Z. Kovacs, and I. Rodriguez, "Path loss, shadow fading, and line-of-sight probability models for 5G urban macro-cellular scenarios," in *IEEE Globecom Workshops*, pp. 1–7, 2015.

[24] P. Swerling, "Probability of detection for fluctuating targets," *IRE Transactions on Information Theory*, vol. 6, no. 2, pp. 269–308, 1960.

[25] S. Kurt and B. Tavli, "Path-loss modeling for wireless sensor networks: A review of models and comparative evaluations.," *IEEE Antennas and Propagation Magazine*, vol. 59, no. 1, pp. 18–37, 2017.

[26] E. Turgut and M. C. Gursoy, "Coverage in heterogeneous downlink millimeter wave cellular networks," *IEEE Transactions on Communications*, vol. 65, no. 10, pp. 4463–4477, 2017.